Astrometric Measurements of Triple Star System 15379+3006 STF 1963AB, STF 1963AC

Harker Russell[1], Lindsey Miller[1], Alexander Beltzer-Sweeney[1,2],
Trey Shilts[1], and Irena Stojimirovic[1,2]

1 San Diego Mesa College, San Diego, California, USA
2 Boyce Research Initiative and Education Foundation (BRIEF)

Abstract: Research team PRSM reports astrometric measurements of the double star system WDS 15379+3006 (STF 1963AB, STF 1963AC) obtained using the iTelescope Network. By performing CCD astrometry, the team determined a position angle of 298.4° ± 0.1° with an angular separation of 05. 28" ± 0.1" for STF 1963AB, and a position angle of 116.1° ± 0.1° with an angular separation of 32.35" ± 0.1" for STF 1963AC. The angular separation and position angle have changed from previous measurements.

Introduction

The purpose of this paper was to select a double star system from the Washington Double Star Catalog (WDS) and observe it using CCD imaging. From the images, we could determine the position angle and separation between stars in the double system. The goal was to determine, based on the orbital plot, if the stars belong to the gravitationally bound system or they are not physically connected and just appear close together.

The star system was selected using the following criteria: a difference in magnitude of no more than 6, with both stars being brighter than 12 magnitudes. A minimum angular separation of 6 arc seconds was also required. In addition, the system must be observable in the spring. Enough historical data on the double star system must exist and will be combined with our measurements to determine if the system is a physical double or visual double star system. Despite the secondary star having a magnitude of 13.58, the triple star system STF1963AB/STF1963AC adhered to the rest of the requirements and the system was selected for observation, Figure 1.

STF1963AC is in the constellation of Corona Borealis and was first observed by Sherburne Wesley Burnham in 1908 (Mason 2017). There have been three more observations made since; the most recent was made in 2009. The separation in 1908 was 31 arc seconds (31"), and 32" in 2009. The position angle has remained virtually unchanged from 116° (Mason 2017).

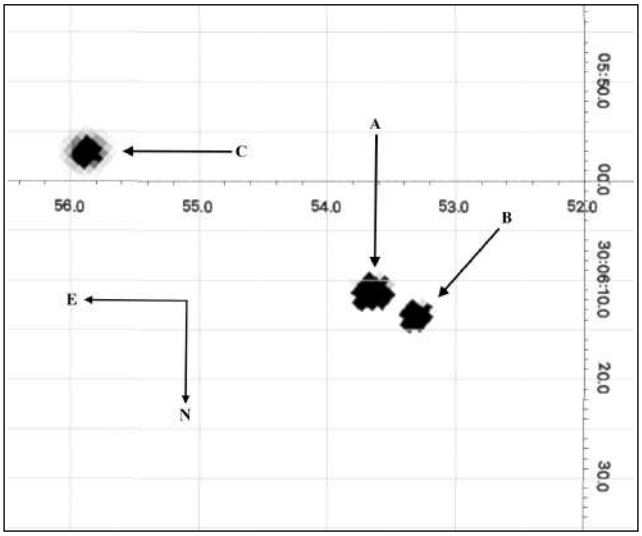

Figure 1. WDS 15379+3006 composite image of A B and C components serves to illustrate the relative positions of each; (WCS). This does not represent relative apparent luminance. The horizontal axis is right ascension (hours). Vertical axis is declination (degrees). Created with SAOImage DS9 (SAOImage, 2016).

The relative proper motion (rPM) is 0.19 arcseconds per year ("/yr)—a good indication that this system has potential to be a gravitationally linked binary star system (Stelle 2017).

The AB component of this system is also very interesting because the rPM is 0.43"/yr which could indicate no gravitational link. The primary star has a magnitude of 8.54 and the secondary star, a magnitude of 8.85. The first separation was 4.2" and the last separation was 5.1" (Mason 2017). The first position angle was 291° and the last position angle was 298°. One journal listing in particular mentions STF1963AB by an alternate identifier, HD 139569 in their Table 2, which listed stars with the following attributes:

> *The results for the most interesting objects… [their team] found a signature of periodic variations (rotational periods of activity cycles) in 19 stars. Whereas 10 stars show a clear overall trend in Hα with time. (Sissa, E., Gratton, R., Desidera, S., et al.).*

The spectral class of primary star is F and the secondary star is a G class star (Stelle 2017). No orbital solutions had been made to date for either AB or AC relative motion. In the Table 1 we present some of the historical measurements of position angle (θ) and separation distance (ρ) as well as the technique codes for the method used to obtain them.

Equipment, Observations, And Data Analysis Procedures

The iTelescope Network's telescope T18 was used to take CCD images of STF1963AB and STF1963AC. This 0.32-meter f/8.0 reflector telescope is located at the AstroCamp Observatory in Nerpio, Spain (38° 09' North, 002° 19' West) and has a resolution of 0.72 arcseconds per pixel (Moore 2017). Four images were ordered. Two images made use of luminance filters—with exposure times of 30 and 60 seconds—and two used hydrogen-alpha filters—with exposure times of 30 and 90 seconds. All of these images were preprocessed (dark and flat subtraction) by the iTelescope data reduction pipeline. Optimal system altitude and time of observation were determined by the use of SkyX Pro software. Images were scheduled through Boyce-Astro, and taken 2017.229798.

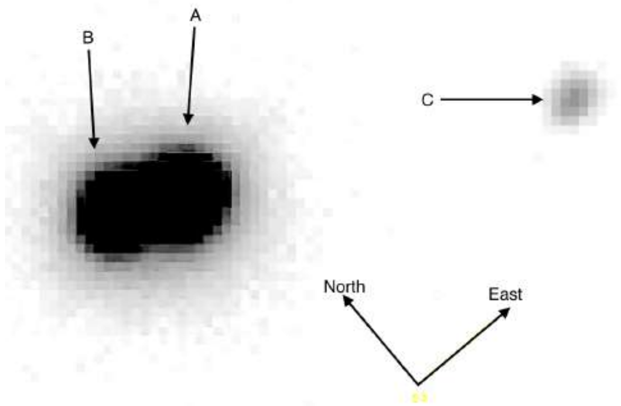

Figure 2. WDS 15379+3006 A B and C components. The purpose of this image is to show the relative apparent luminance of all system components with respect to each other and to demonstrate the difficulties that arose in determining the centroid of component-A when measuring ρ and θ of STF1963AB/ STF1963AC. This necessitated developing a way to double check measurements made in Mira64 that utilized automatic centroid detection (Mira, 2016).

Table 1. *Historical and present measurements for STF 1963 AC (WDS 15370+3006). The WDS (Mason 2017) technique Codes for Table 1 are as follows: Ma, Micrometer with refractor telescope; E2, 2MASS; Eu, UCAC3 or UCAC4; C, CCD image.*

WDS 15379+3006 AC			
Date of Observation	Angle (θ)	Separation (ρ)	Technique Code
1908.31	115.9	31.0	Ma
1998.25	116.3	32.09	E2
2002.154	116.0	31.85	Eu
2009.448	116.4	31.98	C
2017.333	116.09	32.35	C

Each image was received as a FITS file. Astrometry of images was performed using MaxImDL v6 software. In its astrometric measurements, MaxImDL finds all the stars in the image and matches them against cataloged positions for stars in that vicinity (by referencing the UCAC4 catalogue). The calculated mapping is stored as standardized World Coordinate System (WCS) values in the FITS header of each image file.

To analyze the separation (θ) and position angle (ρ) of the components in our triple system Mira64 was used. Due to STF1963AB having such a small Δ magnitude, and STF1963AC Δ magnitude being relatively large, see Figure 2, a process coined 'manual centroid detection' was developed by the team and used for measuring the position angle and separation in addition to the automatic centroid technique provided by Mira64.

The manual centroid detection was carried out as follows: The location of the primary star's (component A) centroid was determined by visual analysis of each pixel in the image, and the RA and Dec of the manually determined centroid was then recorded as shown in Mira64, Figure 3. The secondary star's centroid could then be determined, through the same methodology, while being able to adjust qualitative attributes of each

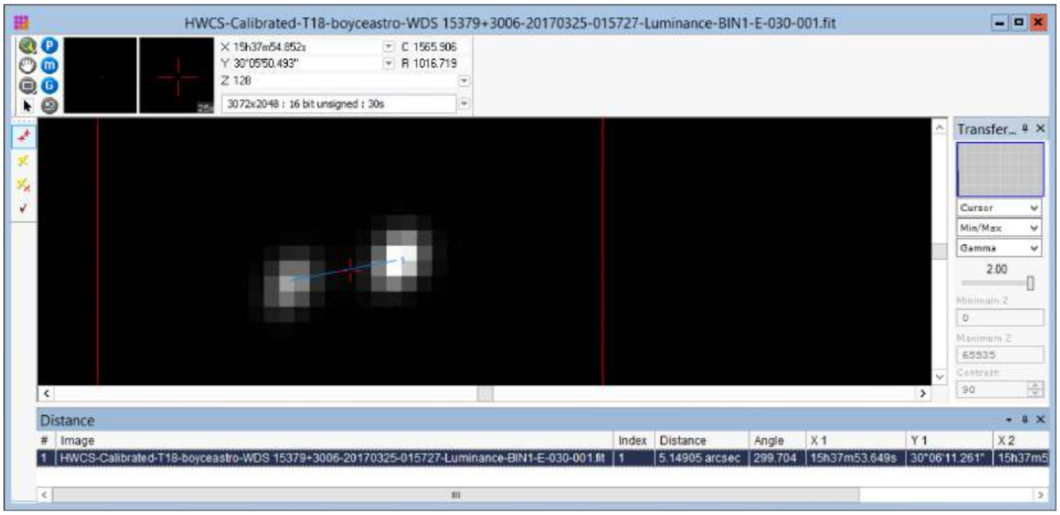

HWCS-Calibrated-T18-boyceastro-WDS 15379+3006-20170325-015727-Luminance-BIN1-E-030-001.fit

X 15h37m54.852s C 1565.906
Y 30°05'50.493" R 1016.719
Z 128
3072x2048 : 16 bit unsigned : 30s

Transfer...
Cursor
Min/Max
Gamma
2.00
Minimum Z 0
Maximum Z 65535
Contrast 90

Distance

#	Image	Index	Distance	Angle	X 1	Y 1	X 2
1	HWCS-Calibrated-T18-boyceastro-WDS 15379+3006-20170325-015727-Luminance-BIN1-E-030-001.fit	1	5.14905 arcsec	299.704	15h37m53.649s	30°06'11.261"	15h37m5

Figure 3. Resolved image of STF1963AB used to determine the coordinates (right ascension and declination) of the primary component-A centroid for use in our manual centroid detection and to measure separation distance (ρ) and position angle (θ) for the STF1963AB component. Differences in accuracy are highlighted in Table 3. This image is created with Mira64 (Mira, 2016).

image to optimally suit the luminance of the secondary star. Mira64's measurement tool was used by dragging the cursor from the previously determined coordinates of component A to the previously determined coordinates of the secondary star. This was done to acquire data points that were not biased by bleed from the nearby A and B components of the system, which the team believed may be biasing the auto centroid centering feature. This process was repeated in each image for all components. Mira64's auto centroid centering feature was also used for measuring separation distances and position angles.

Regarding the STF1963AC component measurements, both automatic and manual centroid detection, Figure 4, techniques had no significant difference between reported data. Both sets of data were, therefore, taken into account, Table 3, for statistical analysis to provide accurate resultant measurements. For STF1963AB, however, measurements made using manual centroid detection were selected for analysis, and this will be discussed in results section.

Using SAOImage DS9 (SAOImage 2016) we were

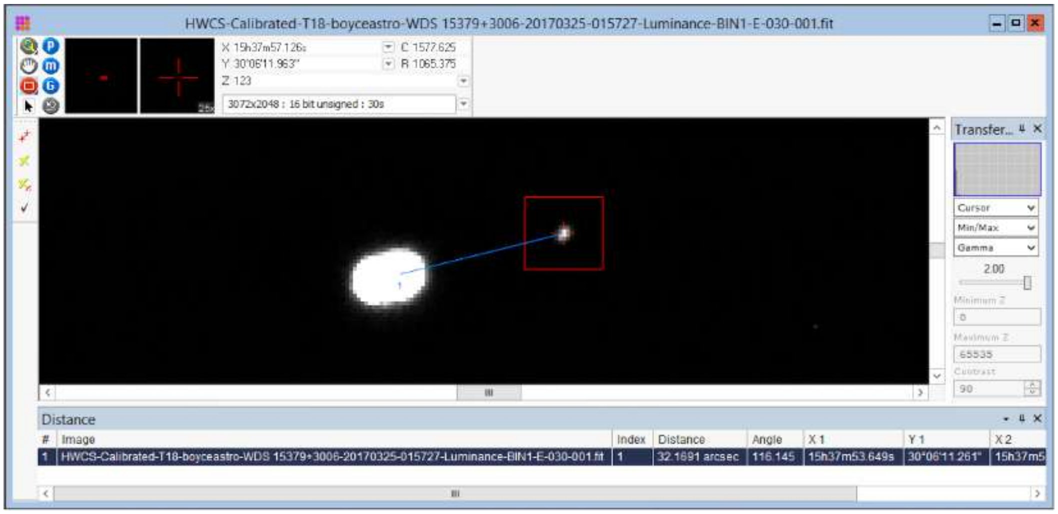

HWCS-Calibrated-T18-boyceastro-WDS 15379+3006-20170325-015727-Luminance-BIN1-E-030-001.fit

X 15h37m57.126s C 1577.625
Y 30°06'11.963" R 1065.375
Z 123
3072x2048 : 16 bit unsigned : 30s

Transfer...
Cursor
Min/Max
Gamma
2.00
Minimum Z 0
Maximum Z 65535
Contrast 90

Distance

#	Image	Index	Distance	Angle	X 1	Y 1	X 2
1	HWCS-Calibrated-T18-boyceastro-WDS 15379+3006-20170325-015727-Luminance-BIN1-E-030-001.fit	1	32.1691 arcsec	116.145	15h37m53.649s	30°06'11.261"	15h37m5

Figure 4. The same image as in Figure 3 after being adjusted to measure separation distance (ρ) and position angle (θ) of STF1963AC. The coordinates (right ascension and declination) of the primary component-A centroid, found using manual centroid technique, were used to ensure that our results would not be skewed by lack of resolution of STF1963AB once STF1963AC was made visible. This image is created with Mira64 (Mira, 2016).

able to check that detection of all three stars were significant with high signal-to-noise ratio using Luminance filter with both 30 and 60 and Hα 90 seconds exposure times. We have failed to detect C component in Hα image with 30 seconds exposure. Table 2 summarizes these findings and Figures 5 and 6 show relative quality of the data taken with these two different filters.

Results

The results of our measurements using both manual centroid and auto centroid techniques are summarized in Table 3. Filter and exposure times are noted as well.

AC Component

Standard deviation of the mean was 0.14 and 0.18 in position angle and separation distance respectively. Precision in the astrometric measurements taken were excellent, as evidenced by 0.07 and 0.05 standard deviation from the mean in separation distance and position angle respectively. Thus the major uncertainty in our data comes from the telescopic resolution of 0.72 arcsec/pixel.

Table 2. *Table of all images taken for PRSM and the signal-to-noise ratio for each component. Determined by using DS9 software to compare the average pixel intensity across the star with average pixel intensity of surrounding pixels (SAOImage, 2016).*

WDS 15379+3006 Signal:Noise Ratio			
Image	**C**	**B**	**A**
Lum 30 sec	58.511	69.739	105.818
Lum 60 sec	106.293	92.597	145.188
Ha 30 sec	NaN	65.600	87.836
Ha 90 sec	28.832	199.681	289.217

With respect to the AC component of WDS 15379+3006, PRSM measurement appears reasonable

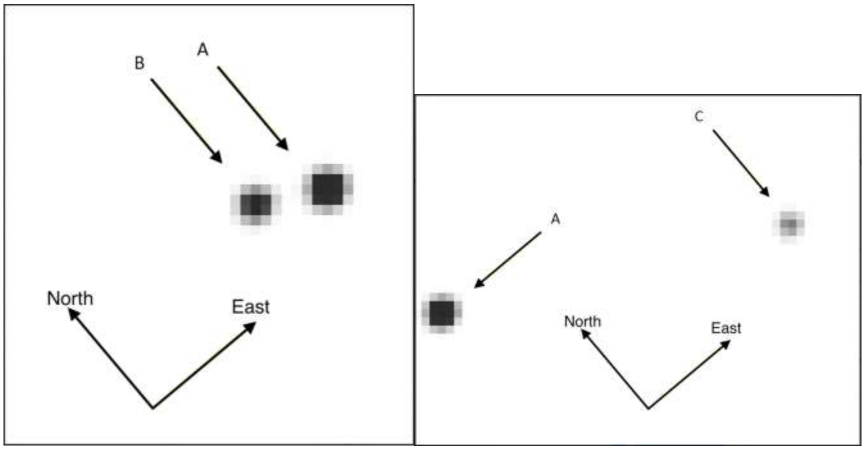

Figure 5. WDS 15379+3006, STF1963AB resolved (left) and STF1963AC resolved (right). These images were obtained using Luminance filter with an exposure of 60 seconds (Mira 2016).

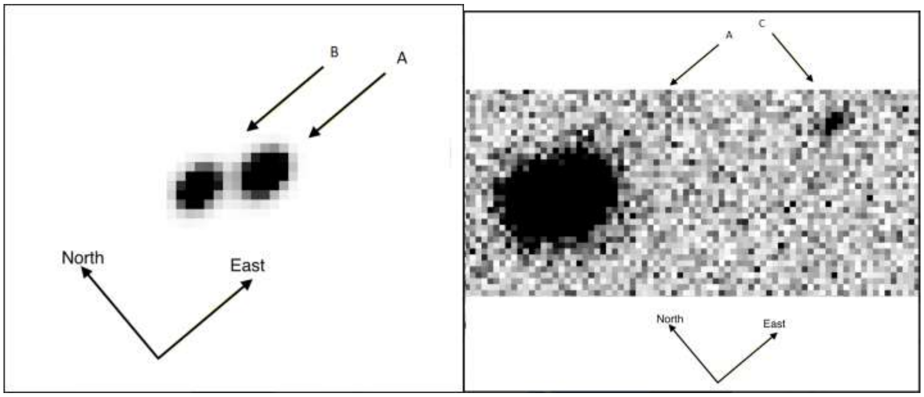

Figure 6. WDS 15379+3006, STF1963AB resolved (left) and STF1963AC (right). These images were obtained using Hα filter with an exposure of 90 seconds (Mira, 2016). As one can see, the A and B components readily bled into one another, necessitating the development of techniques other than automatic centroid detection for our measurements (detailed below).

Table 3. *Data table of all measurements taken of STF 1963 (AC and AB components). All measurements were used to tabulate average, median, standard deviation, and standard deviation of the mean, except those with labeled with a "*" which were omitted. These measurements were found to lie demonstrably outside of the trends outlined by previous measurements and those that used the Manual Centroid Detection techniques. Measurements of Separation (ρ) in STF1963AB were found to be significant when compared to trends (see Figure 11) and therefore the Automatic Centroid Measurements were omitted. Average values were used as results and plotted below.*

WDS 15379+3006					
* omitted from statistics and plots		AC component		AB component	
	Image filter (exposure time)	Separation (Rho)	Angle (Theta)	Separation (Rho)	Angle (Theta)
Auto Centroid	Luminance (30 sec)	32.5615	116.2550	4.2853*	298.0100
	Luminance (60 sec)	32.4889	116.1980	4.1497*	299.0020
	Hydrogen Alpha (30 sec)	NaN	NaN	4.2320*	299.2580
	Hydrogen Alpha (90 sec)	32.4194	115.9810	4.2540*	297.7390
Manual Centroid	Luminance (30 sec)	32.1691	116.1450	5.1491	299.7040
	Luminance (60 sec)	32.3999	115.8320	5.2204	298.3200
	Hydrogen Alpha (30 sec)	NaN	NaN	5.3799	297.2150
	Hydrogen Alpha (90 sec)	32.0435	116.1130	5.3677	297.6860
Statistical Analysis	Average:	32.3471	116.0873	5.2793	298.3668
	Median:	32.3999	116.1130	5.2204	298.0100
	Std Deviation:	0.1816	0.1419	0.0979	0.8139
	Std Deviation of the Mean:	0.0687	0.0536	0.0438	0.2713

when compared with historical measurements (see Figures 8 and 9) that will be explored in greater detail in the discussion section.

AB Component

With respect to the AB component of WDS 15379+3006, the astrometric measurement appears reasonable when compared with historical measurements, Figures 10 and 11. Standard deviation of the mean between all manual centroid measurements of this system were 0.8 and 0.1 in position angle and separation distance respectively, Table 3. Precision in the astrometric measurements taken were also excellent, as evidenced by 0.3 and 0.04 standard deviation from the mean in position angle and separation distance respectively.

While there was no significant difference in position angle determination between automatic versus manual centroid detection methods, Figure 11 demonstrates that a separation distance near four arc-seconds

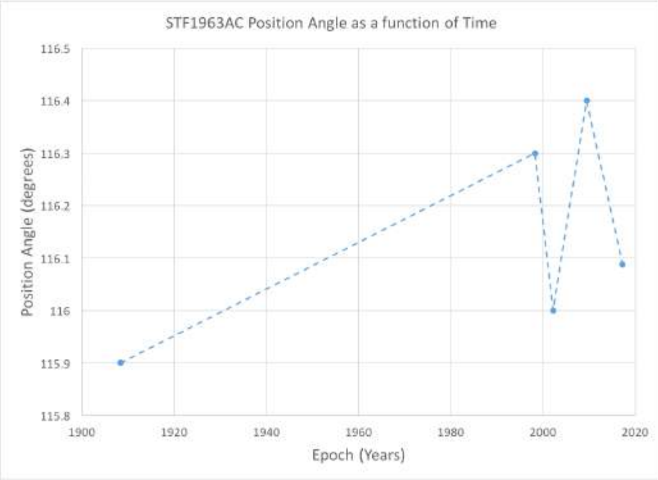

Figure 8. Graphical depiction of all measurements of position angle (to date) of STF1963AC with respect to time (epoch).

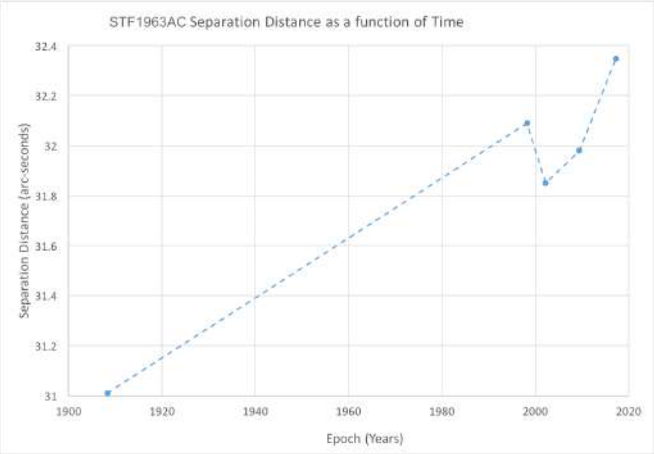

Figure 9. Graphical depiction of all measurements of separation distance (to date) of STF1963AC with respect to time (epoch).

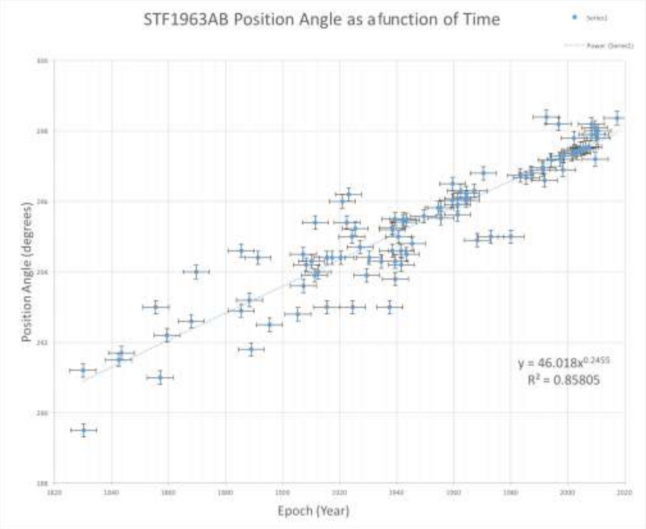

Figure 10. Graphical depiction of all historical measurements of position angle (to date) of STF1963AB with respect to time (epoch). One can see a linear trend, not indicative of an orbital binary. Outliers omitted.

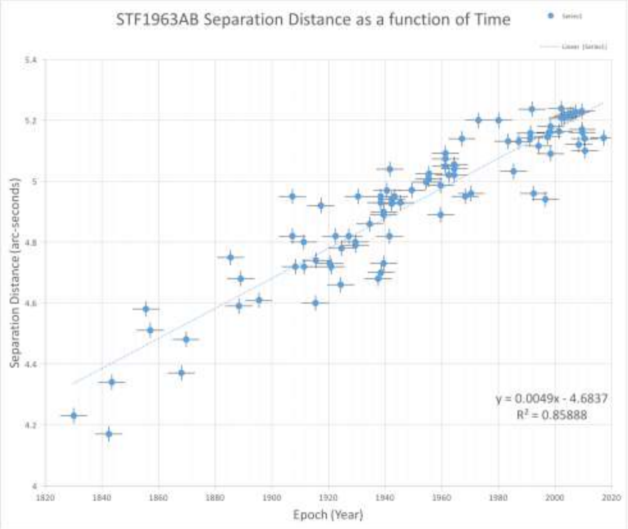

Figure 11. Graphical depiction of all measurements of separation distance (to date) of STF1963AB with respect to time (epoch). Again, one can see a linear trend, not indicative of an orbital binary. Outliers omitted.

clearly does not follow the historic trend outlined therein. Manual centroid detection methods, however, did yield precise measurements which fit this trend nicely. Furthermore, a significant difference between measurements which used manual centroid detection and those that used automatic centroid detection did occur, and the measurements which utilized manual centroid detection techniques had a high degree of precision with respect to one another between images (Table 3). For this reason, measurements of separation ascertained by utilizing automatic centroid detection were omitted from AB considerations.

Discussion

AC Component

When compared with historical observational data half a degree variation in position angle between measurements of 1908 and 2009 is seen. Somewhat zigzagged pattern in position angle changes is observed, Figure 8. The 2017 angular separation measurement shows 1.4 arc second change compared to the first historic measurement. Within the last twenty years of measuring the overall change in the separation angle is within our resolution limit, Figure 9. Thus, no reasonable trend could be ascertained by careful analysis of the position angle or separation distance with respect to their epoch.

Orbital plots of C component's position relative to A, Figure 12, does not yield any further evidence of a gravitational relationship between the two components either (Genet 2016). Although only five astrometric measurements have been contributed to-date they all show very good overall agreement, Figure 12 right panel, leading us to conclude that C component doesn't appear to move significantly with respect to the A component, Figure 12, left panel.

AB Component

When compared with historical observational data, this system shows consistency, Figures 10 and 11. Since the first measurements were taken in early 1800s the position angle has changes by eight degrees and the separation has changed by only one arc-second. This indicated that the distance between A and B stars has not change significantly in the last two hundred years while they did change position with respect to each other.

In the Figure 13, we have attempted to present orbital motion of component B with respect to the component A. In the left panel, the A component is found in the origin and all historic data for the motion of component B are plotted including our measurement. In the right panel we averaged measurements in 60-year bins to clarify any trends in motion. Although no elliptical orbit has yet been made available, more observations of this system, over some time, may be able to provide enough data to establish one. This statement is justified by an apparent curvature toward the north-northeast in the motion of component B with respect to the component A. A determination as to whether or not STF1963AB is an optical double or long-period gravi-

(Text continues on page 249)

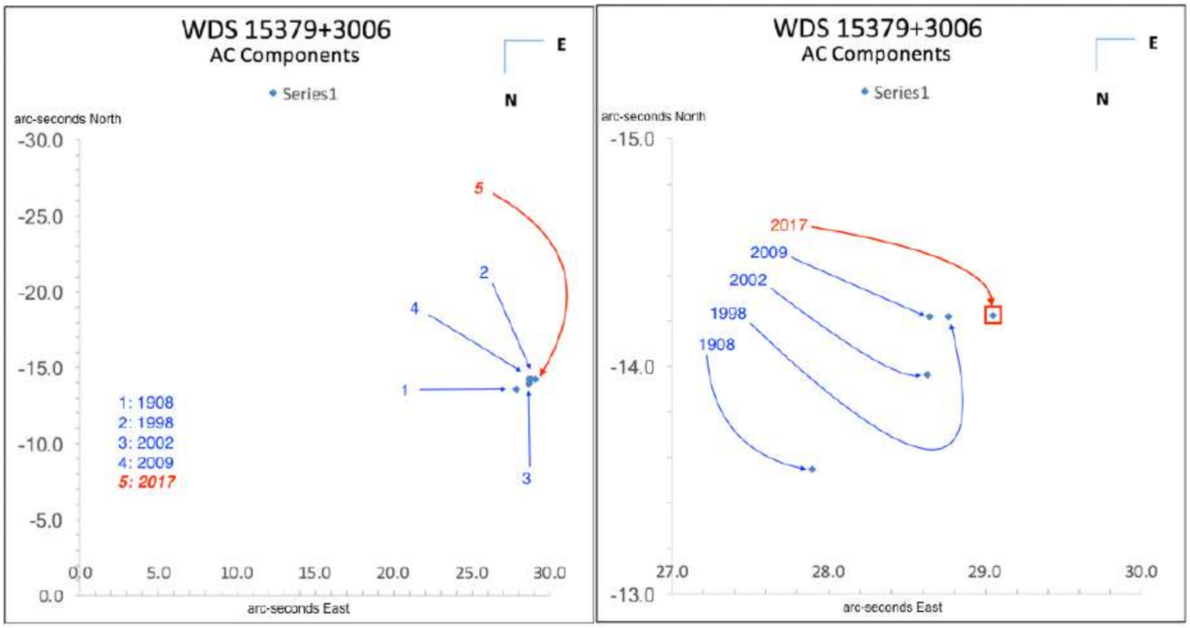

PM: -023+023 -019+028 **PM: -023+023 -019+028**

Figure 12. Graphical depiction of historical measurements (C component) and present measurement of STF1963AC. Team PRSM measurement appears in red, and by italicized text. In the left panel STF 1963's A component is at the coordinate system origin. In the right panel we zoom into the motion of C component to capture the positions relative to one another.

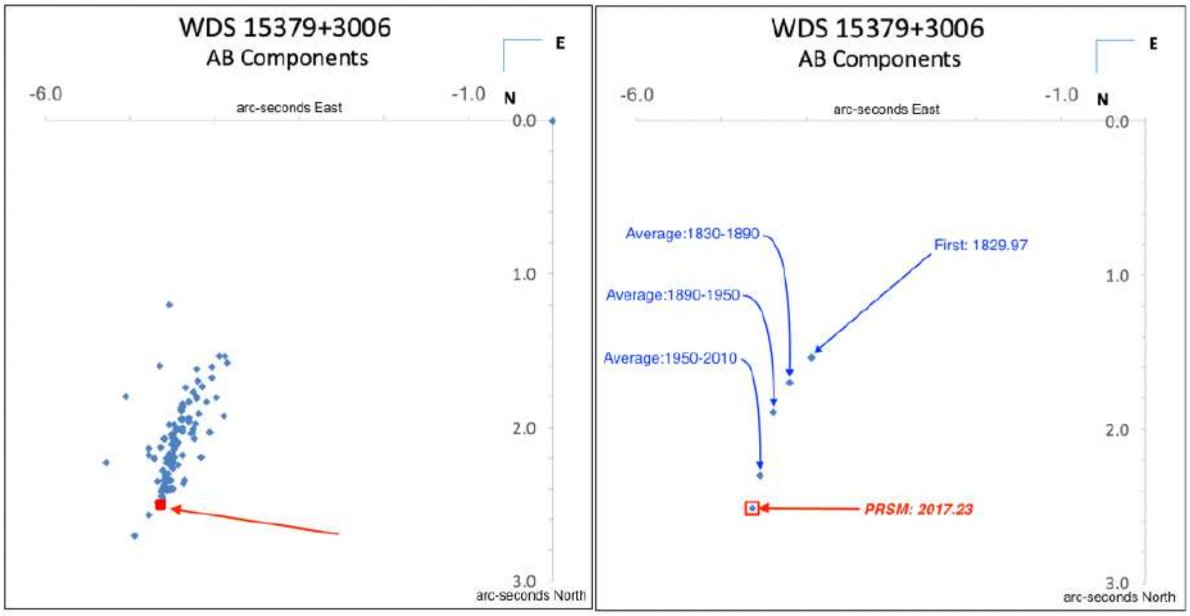

PM: -023+023 -042+038 **PM: -023+023 -042+038**

Figure 13. Graphical depiction of historical measurements and present measurement of STF1963AB. A component positioned at the origin (left panel). Team PRSM measurement appears as a red square, and indicated by an arrow. On the right panel graphical depiction of historical measurements, averaged in 60-year swaths of measurements to clarify any trends in motion. Team PRSM measurement appears and encircled by a red square, and italicized text.

(Continued from page 247)

tational binary is difficult to make as both of these can exhibit this overall linear behavior (Heintz 1978).

Conclusion

Precise measurements of WDS 15379+3006 (STF1963AB and STF1963AC) were obtained successfully from four CCD images taken by iTelescope networks T-18 telescope located in Nerpio, Spain. These measurements shall contribute to a large body of historical astrometric measurements of STF1963AB, and to the very few historical astrometric measurements of STF1963AC. STF1963AC shows no reasonable trends and it is the opinion of the authors that it is a visual double star system, and not a physical double star system as suggested by its low rPM.

Measurements of the STF1963AB component of WDS 15379+3006 show a linear trend, although there may be some reason to argue that a seemingly curved path of B with respect to the A exists and therefore is evidence for a long period gravitationally bound system, no orbital relationship was able to be ascertained at the time of this study.

Acknowledgements

The authors would like to thank the iTelescope Network for the use of their service and the United States Naval Observatory for providing historical measurement data. The authors would also like to thank the Boyce Research Initiative and Education Foundation (BRIEF) for their generous financial donation that allowed us to use the iTelescope robotic telescope system, remote server and software. Lastly, the authors thank Pat Boyce, Grady Boyce and Russell Genet for their guidance and expertise during the review of this paper.

References

Genet, R., Johnson, J., Buchheim, R., and Harshaw, R., 2016, *Small Telescope Astronomical Research Handbook.*

Hartkopf, W.I., Mason, B.D., and Wycoff, G.L., 2011, "Speckle interferometry at the U.S. Naval observatory", *The Astronomical Journal,* **3**, pp. 3.

Heintz, W.D., 1978, *Double Stars.* Dordrecht: D. Reidel Publishing Company, pp. 17-18.

Mason, B., "The Washington Double Star Catalog", 2017, Astrometry Department, U.S. Naval Observatory. http://ad.usno.navy.mil/wds/Webtextfiles/wdsnewframe3.html

MaxIm DL [Computer software], 2017, Diffraction Ltd., Retrieved from http://diffractionlimited.com/product/maxim-dl/.

Mira Pro x64 [Computer software], 2016, Mirametrics Inc., Retrieved from http://www.mirametrics.com/mira_pro_x64.php.

Moore, B.. 2017, iTelescope-T18-Medium Deep Space -Spain, iTelescope.Net Pty Lt. http://www.itelescope.net/telescope-t18/.

SAOImage DS9 [Computer software], 2016., Smithsonian Astrophysical Observatory., Cambridge, MA., Retrieved from http://ds9.si.edu/site/Download.html.

Sissa, E., Gratton, R., Desidera, S., Martinez Florensano, A.F., Bonfanti, A., Carolo, E., Vassollo, D., Claudi, R.U., Endl, M., and Cosentino, R., 2016, "Hα- activity and ages for stars in the SARG survey", *Astronomy and Astrophysics.* pp. 7-8.

SkyX Pro [Computer software], 2017, Software Bisque Inc., Retrieved from http://www.bisque.com/sc/media/24/default.aspx.

Stelle Doppie. 15379+3006 STF1963AC., 2017, http://stelledoppie.goaction.it/index2.php?menu=29&iddoppia=63379.